

**Figure 1.** PXRD patterns of the substituted nickel oxide cathodes. (a)  $\text{LiNi}_{0.7}\text{B}_{0.3}\text{O}_2$ , (b)  $\text{LiNi}_{0.7}\text{Al}_{0.1}\text{B}_{0.2}\text{O}_2$ , (c)  $\text{LiNi}_{0.7}\text{Al}_{0.2}\text{B}_{0.1}\text{O}_2$ , (d)  $\text{LiNi}_{0.7}\text{Al}_{0.3}\text{O}_2$ , and (e)  $\text{LiNiO}_2$ . Inset: XRD of  $\text{LiNi}_{0.7}\text{B}_{0.3}\text{O}_2$  heated at  $750^\circ\text{C}$  for 2 h.

ume were determined by an iterative least squares refinement method using the indexed  $h$ ,  $k$ ,  $l$  values and are included in Table I.

A low extent of substitution of larger cations by B is expected to result in the contraction of unit cell parameters.<sup>18</sup> Interestingly, in

the present study also, a decreasing trend in  $a$  value has been observed with the increasing B content. The degree of trigonal distortion of the cubic lattice, normally expressed as the  $c/a$  ratio was also found to be reduced for the doped derivatives of  $\text{LiNiO}_2$ . These reduced unit cell parameters may also be viewed as an impact of location of dopants in the compound *i.e.*, if the B atoms are located in crystallographic sites exactly the same as that occupied by the constituent atoms in the stoichiometric  $\text{LiNiO}_2$ , reduction in cell volume may be expected. Boron when substituted isomorphically for Ni in the  $3a$  octahedral ( $-3m$ ) sites of the  $\text{NiO}_2$  layers may lead to significant changes in the very appearance and the intensity of the diffraction lines. However, it is also reported in the literature<sup>18</sup> that the low scattering power (and the low proportion) of B may not be helpful in finding the exact location of these atoms by XRD. Therefore, we do not attribute the observed change in the appearance as well as the intensity of the diffraction peaks solely to the entire occupation of all the substituted B atoms in to the octahedral ( $-3m$ ) sites of the  $\text{LiNiO}_2$  crystal lattice.

On the other hand, the  $c$  value was found to decrease initially up to 10% of B content and thereafter an increase in the  $c$  values has been noticed with the increasing B content. This may be due to the combined effect of the smaller radius of boron that could not effectively influence the surrounding oxygen spheres to result in a smaller lattice constant value throughout the series in a linear fashion and the possible tetrahedral  $3m$  site occupancy of part of the boron doped in the  $\text{LiNiO}_2$  crystal lattice. Also, the overall effect of the substitution with Al and B may be a probable reason for the difference in the trend observed with the simultaneous doping of Al and B with an increasing B content and a lesser Al content. The  $c/a$  ratio, which is a qualitative measure of the stabilization of  $\text{Ni}^{+3}$  and the 2D layered structure<sup>24</sup> of the compounds has been found to vary between 5.007-4.956, substantiating the structural stability of the synthesized compounds. Similarly, the values of  $I_{(003)}/I_{(104)}$  ratio vary between 1.11 (for  $\text{LiNi}_{0.7}\text{Al}_{0.3}\text{O}_2$ ) to 1.27 (for  $\text{LiNi}_{0.7}\text{Al}_{0.1}\text{B}_{0.2}\text{O}_2$ ), a qualitative measure for the better battery activity of the compounds.<sup>24</sup> Also, the unit cell volumes calculated for the compounds indicate volume shrinkage as the B content increased.

It has been reported that the presence of extra nickel as impurity in the form of electrochemically inactive  $\text{Ni}^{2+}$  in the  $3b$  Li sites of  $\text{LiNiO}_2$ , is responsible for the reduced electrochemical performance of the same. Delmas *et al.*<sup>25</sup> have ascribed the capacity fading to the possible formation of electrochemically inactive region in the cathode material, resulting from the oxidation of pre-existing  $\text{Ni}^{2+}$  ions in the lithium layer. In this context, it is quite interesting that the extra nickel in the lithium plane can partially be solved by B substitution. Further, in the recent investigations of Alcántara *et al.*,<sup>18</sup> it is reported that the presence of a B dopant in the  $\text{LiCoO}_2$  compound favored lattice adaptation to a super lattice structure of lithium ions. Similarly, it is believed that the presence of boron in the tetrahedral sites of  $\text{LiNiO}_2$  (an analog of  $\text{LiCoO}_2$ ) makes the structure more flexible with respect to lithium ordering. In other words, the boron dopant may displace  $\text{Ni}^{2+}$  to  $3a$  sites, leading to an increased  $\text{Ni}^{3+}$  content in the boron-doped nickel oxides, thus enhancing the electrochemical activity. This has further been substantiated by the observations of Kemp and Cox,<sup>26</sup> who have reported the presence of relatively increased amount of  $\text{Ni}^{3+}$  ions in the  $3a$  sites of  $\text{LiNiO}_2$  resulted from the germanium doping. Hence the boron substitution in the present series of compounds favors this kind of stabilization of  $\text{Ni}^{+3}$  in the  $3a$  sites, forcing away the  $\text{Ni}^{2+}$  that was originally present in the  $3b$  lithium sites, thus resulting in the stabilized 2D layer structure ultimately. This is further evidenced by the higher  $I_{(003)}/I_{(104)}$  ratio values of 1.25 and 1.27, calculated for the 10 and 20% of boron, respectively. Hence the substitution is facilitated even at a moderate temperature of about  $600\text{--}700^\circ\text{C}$  despite the difference in the ionic sizes of  $\text{Ni}^{3+}$  (0.56 Å),  $\text{Al}^{3+}$  (0.51 Å) and  $\text{B}^{3+}$  (0.24 Å), thus establishing the solubility of  $\text{Al}^{3+}$  and  $\text{B}^{3+}$ .

The effect of Al cannot be explained completely by XRD, because it is already reported that the aluminum ions do not perturb the layered structure of the compound.<sup>13,16,27</sup> However, based on the reported results of  $^{27}\text{Al}$  magic angle spinning nuclear magnetic resonance,<sup>13</sup> a possible occupancy of aluminum ions in the octahedral sites (3a) and a smaller amount of Al in the tetrahedral 6c sites are expected to occur in the present case also. Though it seems to be uncertain to describe the exact location of Al from XRD, it is further understood from the forthcoming characterization studies such as FTIR and CV that the possible occupancy of interstitial 6c sites by a lesser fraction of Al cannot be neglected. Also, it is worthwhile to remember that the interstitial tetrahedral site occupancy of Al, if any, could lead to negative effect only with respect to lithium diffusion in the aluminum-substituted solid solutions.<sup>13</sup> This is reflected in the charge/discharge studies, wherein a 20% reduction in capacity, observed for the  $\text{LiNi}_{0.7}\text{Al}_{0.3}\text{O}_2$  compound over 25 cycles, is apparently due to the hindered lithium diffusion.

Since boric acid has a lower melting point ( $170^\circ\text{C}$ ), it is highly probable for the formation of Li—B—O glass like compounds in the final products. The formation of such type of material would definitely impart hardness and the crystallinity of the products would be affected, despite the fact that glasses do not have long-range crystallographic order. Since the products are soft and fluffy and are of high crystalline in nature, we preclude the possibility of glass formation in the final oxides.

**Local structure by FTIR analysis.**—The presence of B and Al as dopants in the  $\text{LiNiO}_2$  lattice can be identified from the IR spectral bands observed for the  $\text{LiNi}_{0.7}\text{Al}_x\text{B}_y\text{O}_2$  solid solutions. Figure 2 a-e shows the FTIR spectrum of the substituted and the unsubstituted nickelate compounds synthesized under the heat-treating condition as mentioned in Table I.

It is understood from XRD observations, that the average bond length between the transition metal ion and the oxygen ions in the  $\text{MeO}_6$  octahedra having a local  $O_h$  symmetry has been decreased as a function of  $y$  in  $\text{LiNi}_{0.7}\text{Al}_x\text{B}_y\text{O}_2$ . This is further supported by the shift in the FTIR spectral bands for the substituted solid solutions when compared to the normal vibrational modes of the unsubstituted nickel oxide that are present around  $400\text{--}700\text{ cm}^{-1}$  region. Peaks around  $860$  and  $1430\text{ cm}^{-1}$  are observed invariably for all the compounds, an indication of the presence of Ni—O bond. The IR spectrum of undoped  $\text{LiNiO}_2$  shows two peaks around  $511$  and  $860\text{ cm}^{-1}$ , which are shifted to lower and higher wave numbers respectively, when doped suitably with B or Al or B and Al. Note that when  $\text{LiNiO}_2$  is substituted either by B or Al, a shift in the peak at  $511\text{ cm}^{-1}$  to lower wavelengths has been observed. On the contrary, when  $\text{LiNiO}_2$  is simultaneously substituted with both B and Al, a shift to higher wavelengths is noted. The dopants may induce changes in  $\text{NiO}_2$  vibrations thus substantiating the fact that the dopants occupy mainly the  $\text{NiO}_2$  slabs. However, the reverse trend observed for the bisubstitution may be due to the combined effects of B and a probable interstitial tetrahedral occupancy of lesser fraction of Al. Typical bands around  $1436\text{ cm}^{-1}$  and  $668\text{ cm}^{-1}$  may be attributed to the effect of B and Al in terms of B—O bond stretching vibrations and Al—O bond vibrations, respectively. Thus the existence of a series of solid solutions *viz.*,  $\text{LiNi}_{0.7}\text{Al}_x\text{B}_y\text{O}_2$  has been understood from IR spectral studies also.

**Other physical properties.**—BET surface area was estimated to be around  $25$  and  $15\text{ m}^2/\text{g}$  for  $\text{LiNi}_{0.7}\text{B}_{0.3}\text{O}_2$  and  $\text{LiNi}_{0.7}\text{Al}_{0.3}\text{O}_2$ , respectively. Due to the fine and foamy nature of the products, the estimated powder density of the compounds were found to be about 70–80% of the theoretical density values, which is commonly observed for the combustion derived products.<sup>28</sup> SEM images captured under the same magnification (400 times) for  $\text{LiNi}_{0.7}\text{B}_{0.3}\text{O}_2$  and  $\text{LiNi}_{0.7}\text{Al}_{0.3}\text{O}_2$  samples are shown in Fig. 3 (a and b), respectively. It is evident from the micrographs that the particles of the former sample with boron as the substituent were of submicrometer size

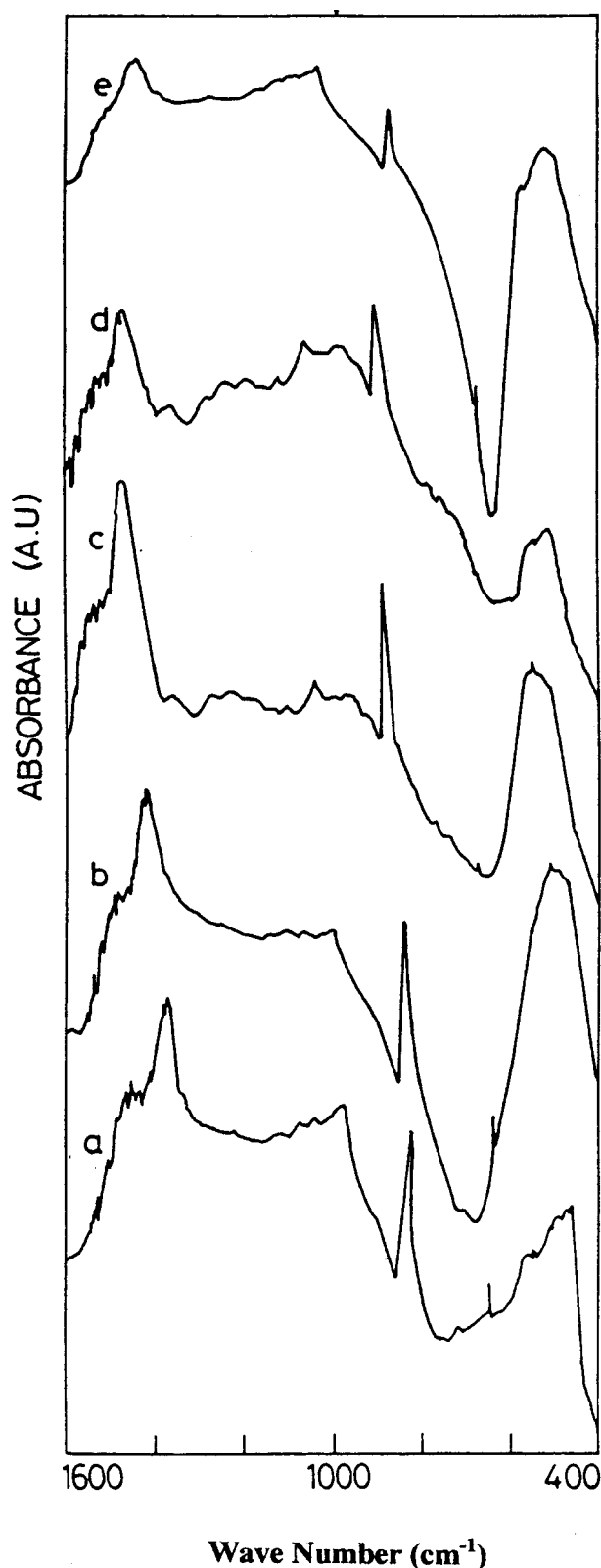


**Figure 2.** FTIR spectra of (a)  $\text{LiNi}_{0.7}\text{B}_{0.3}\text{O}_2$ , (b)  $\text{LiNi}_{0.7}\text{Al}_{0.1}\text{B}_{0.2}\text{O}_2$ , (c)  $\text{LiNi}_{0.7}\text{Al}_{0.2}\text{B}_{0.1}\text{O}_2$ , (d)  $\text{LiNi}_{0.7}\text{Al}_{0.3}\text{O}_2$ , and (e)  $\text{LiNiO}_2$ .

whereas for the latter compound with Al as the substituent, the particles were slightly higher in dimension. For the samples  $\text{LiNi}_{0.7}\text{Al}_{0.2}\text{B}_{0.1}\text{O}_2$  and  $\text{LiNi}_{0.7}\text{Al}_{0.1}\text{B}_{0.2}\text{O}_2$ , the size of the particles was found to be almost similar to that of  $\text{LiNi}_{0.7}\text{Al}_{0.3}\text{O}_2$ . From this

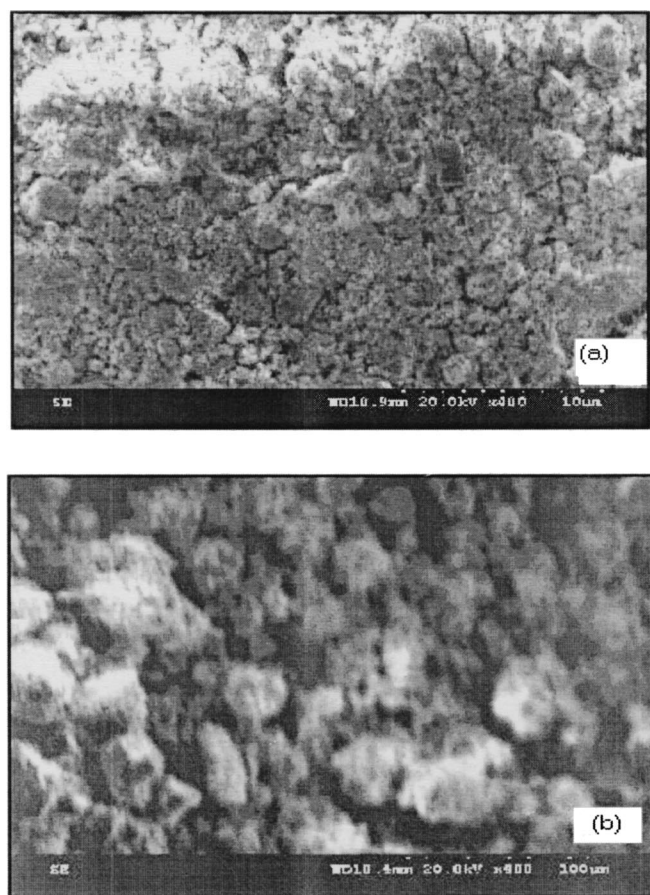


Figure 3. SEM of  $\text{LiNi}_{0.7}\text{Al}_{0.3}\text{O}_2$  and  $\text{LiNi}_{0.7}\text{B}_{0.3}\text{O}_2$ .

observation, we may conclude that the presence of aluminum as dopant may very well be correlated with the size of the particles, *i.e.*, the presence of Al as one of the dopants or as the only dopant has led to the formation of sintered nature of the final product. As a result, the size of the particles was found to be slightly higher than that of the corresponding boron-substituted derivative. This has further been confirmed from the lower BET surface area values ( $15 \text{ m}^2/\text{g}$ ), determined invariably for all the aluminum-substituted compounds.

### Electrochemical Analysis

**Cyclic voltammetry.**—Figure 4 shows the cyclic voltammogram of  $\text{Li}/\text{LiNi}_{0.7}\text{Al}_x\text{B}_y\text{O}_2$  ( $x + y = 0.3$ ) cells fabricated as 2016 coin type, using a mixture of 1 M  $\text{LiAsF}_6$  in 1:1 v/v of EC and DMC as the electrolyte. The cyclic voltammogram recorded between 3.6 and 4.4 V at a scan rate of 0.1 mV/s indicates that with the increasing boron content, the anodic current decreased and a broad maximum at 4.1–4.3 V was observed. On the contrary, cathodic peak current at lower voltage region started diminishing and the peak at higher voltage region increased as a function of boron content. But for all the samples except  $\text{LiNi}_{0.7}\text{Al}_{0.3}\text{O}_2$ , a significant shift in the reduction peak toward higher voltages has been observed. As a result, the voltage difference between anodic and cathodic peaks has been narrowed down which is an indication of the high  $\text{Li}^+$  reversibility. On the contrary, the large difference between the anodic and cathodic peaks observed for the  $\text{LiNi}_{0.7}\text{Al}_{0.3}\text{O}_2$  may be attributed to the partial occupancy of Al in the interstitial 6c sites of nickel oxide crystal structure. Therefore, as already mentioned in the XRD analysis, the hindered  $\text{Li}^+$  diffusion due to the interstitial occupancy of Al can thus be understood from the CV studies also.

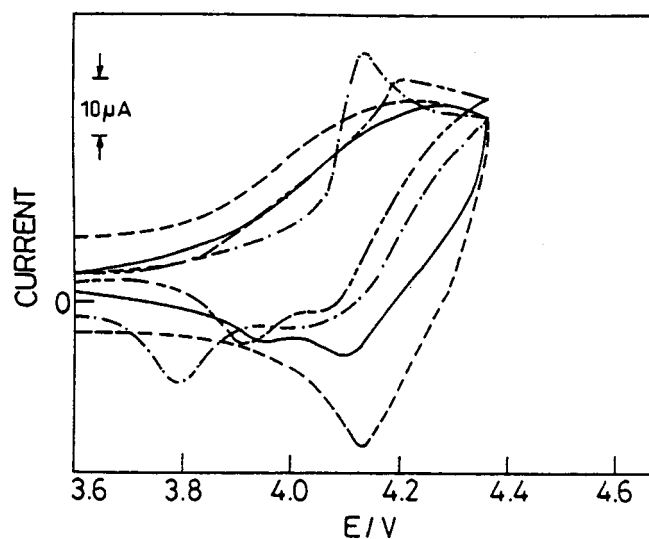


Figure 4. Cyclic voltammograms of the oxide cathodes cycled between 3.6 and 4.4 V at a scan rate of 0.1 mV/s. (---)  $y = 0.3$ , (-·-·-)  $y = 0.2$ , (—)  $y = 0.1$ , and (----)  $y = 0.0$ .

**Charge/discharge cycling studies.**—Charge/discharge cycling has been performed at a current density of  $0.1 \text{ mA}/\text{cm}^2$  between the cutoff voltages of 3 and 4.5 V. Figure 5 shows the cyclability of these samples up to 25 cycles. The cyclability of the cathodes was found to be satisfactory only for the 10 and 20% boron containing lithium nickel oxides, *viz.*,  $\text{LiNi}_{0.7}\text{Al}_{0.2}\text{B}_{0.1}\text{O}_2$  and  $\text{LiNi}_{0.7}\text{Al}_{0.1}\text{B}_{0.2}\text{O}_2$ . This has further been supported by the calculated  $I_{(003)}/I_{(104)}$  ratio value derived from XRD, which was found to be *ca.* 1.3 for these two samples only.

The better cyclability of the doped nickelate derivatives may also be explained from the thermodynamic point of view. Veluchamy *et al.*<sup>20</sup> in their studies with B-doped  $\text{LiMn}_2\text{O}_4$  ascribed the stability of the compound to the high Gibbs energy of formation ( $\Delta G_f^\circ$ ) of  $\text{Mn}_2\text{O}_3$  and  $\text{B}_2\text{O}_3$ . Like wise, the higher  $\Delta G_f^\circ$  values<sup>29</sup> of  $\text{Al}_2\text{O}_3$  ( $-1582 \text{ kJ/mol}$ ) and  $\text{B}_2\text{O}_3$  ( $-1192 \text{ kJ/mol}$ ) are in favor of the stability of the nickel oxide derivatives substituted simultaneously with  $\text{Al}^{3+}$  and  $\text{B}^{3+}$ . The structural stability of the  $\text{LiNi}_{0.7}\text{Al}_x\text{B}_y\text{O}_2$  compounds may also be viewed as a function of bond strength<sup>29</sup> of the respective metal-oxygen bonds. Since the bond strength values of

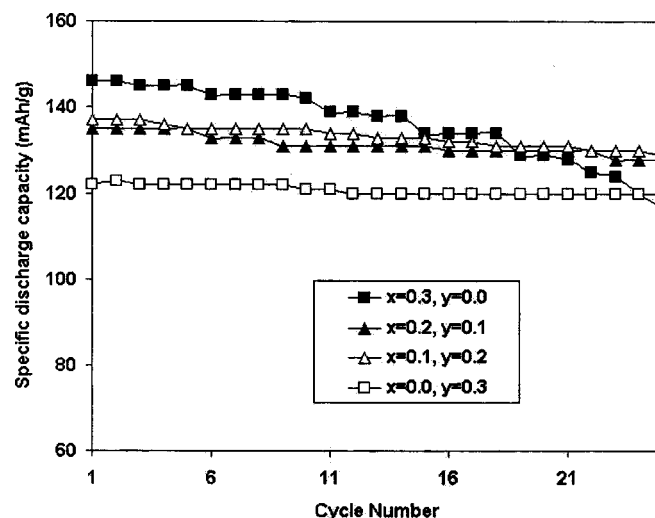


Figure 5. Cyclability of  $\text{Li}/\text{LiNi}_{0.7}\text{Al}_x\text{B}_y\text{O}_2$  cells (scan rate = 0.1 mV/s).

